S0032-3861(96)00495-8

Polymer Vol. 38 No. 2, pp. 339–346, 1997

0032-3861/97/$17.00+0.00

Monte Carlo simulation and self-consistent field theory for a single block copolymer chain in selective solvents

X. F. Yuan*[†,‡] **and A. J. Masters**[†]
[†]*Department of Chemistry, University of Manchester, Manchester M13 9PL, UK and*
[‡]*H. H. Wills Physics Laboratory, University of Bristol, Bristol BS8 1TL, UK*
(Received 28 March 1996)

A self-consistent field (SCF) theory and a Monte Carlo (MC) simulation technique have been developed for block copolymer systems. Calculations were carried out using both SCF theory (with a simple mean-field potential) and MC simulation for an AB diblock copolymer chain for a wide range of solvent conditions. Fairly good agreement between these two methods was found. For an ABA triblock copolymer, a sharp transition between two conformations was observed by MC simulation: in one state conformation the copolymer has two collapsed A globules at either end of the B block chain and in the other state conformation one collapsed A globule comprising of the two A blocks with a loop of the B block chain sticking out. It is our strong suspicion that this would be a true phase transition in the limit of infinite chain length. Copyright © 1996 Elsevier Science Ltd.

(Keywords: Monte Carlo simulation; self-consistent field theory; block copolymer; selective solvents; conformation; phase transition)

INTRODUCTION

The conformational and thermodynamic properties of copolymers depend strongly on interactions between segments as well as on the composition of chains and the flexibility of the blocks. Flexible copolymer solutions exhibit very rich phase behaviour and can undergo micellization and gelation processes as the polymer concentration increases. Extensive experimental work[1–3] has been carried out. In the concentrated regime, cubic, hexagonal, lamellar and other phases have been identified[4,5]. Although there is quite an amount of experimental results, theoretical work[1,2,6–12] and computer simulation[13] on these complicated phase behaviours are still rather limited. The phase behaviour of copolymer solutions depends upon understanding the difference of Gibbs free energy between the chains in a self-assembled state and in an isolated state. In this paper, we focus on studying the behaviour of the isolated copolymer chain in selective solvents.

Among the early work on an isolated copolymer chain was that of Froelich and Benoit[14] who investigated the case where the segments had small excluded volumes so that departures from Gaussian configurations could be analysed via a perturbation expression. The effect of larger excluded volumes on diblock copolymers was explored by Edwards[15] using a self-consistent set of mean field equations. In the special case of equal block lengths ($L_A = L_B$ for the continuous chain model), equal number of segments in each block ($n_A = n_B$) and the interaction parameters (the second virial coefficients) of the segments related by $v_{AA} = v_{BB} = -v_{AB}$, Edwards showed one solution to the mean field equations was a Gaussian distribution for each block, yielding a spherically symmetric density profile centred on the mass centre, but for sufficiently negative values of v_{AA} another solution to the equations was a dumb-bell-like density distribution in which the A chain concentrated in one lobe and the B chain in the other. A phase transition between these two states was predicted. Additional theoretical approaches include the biellipsoidal model calculations of Bendler *et al.*[16–18] in which the A and B chains are modelled as smooth ellipsoidal density clouds. The theory is in basic agreement with the simulation results of Tanaka *et al.*[19–22] and the authors report that for $v_{AA} = v_{BB} = -v_{AB}$, the combination studied by Edwards, rapid conformational changes do occur. Kurata and Kimura[23] present a smoothed-density treatment. The theory, for $n_A = n_B$, predicts the coil-globule collapse if v_{AB} is made more and more negative when $v_{AA} = v_{BB} = 0$, and in the Edwards' case where $v_{AA} = v_{BB} = -v_{AB}$ predicts the collapsed dumb-bell form as did Edwards for sufficiently large and positive v_{AB}. When the theory is applied to the triblock A–B–A chain (with equal numbers of A and B segments) then a collapse transition is predicted in the $v_{AA} = v_{BB} = mv_{AB}$ case, for $m < -2$, with the two A chains coming together. More recent theoretical studies have been carried out using renormalization group techniques both for diblock and triblock copolymers, and good quantitative agreement is claimed between the theoretical results and

---

* Present address: Room 388, Department of Applied Physics, School of Engineering, Nagoya University, Chikusa-ku, Nagoya 464-01, Japan

Monte Carlo simulation [24-26]. These calculations have the great advantage of avoiding many of the approximations that are introduced in more intuitive theories, but unfortunately the theories are largely limited to polymers in good solvents and so do not, as yet, give information about the coil-globule or the segregation transition.

In the present work, we shall apply a self-consistent field (SCF) theory and Monte Carlo (MC) simulation technique in studying the segregation transition of a single block copolymer chain. The MC simulation technique and the SCF theory are presented below. The segregation transitions of a block copolymer chain are discussed later. We shall end with a summary.

MONTE CARLO SIMULATION TECHNIQUE

We consider a linear diblock copolymer of n links, each of length l_0 and connecting an A block of n_a beads to a B block with n_b beads. The chain molecule is modelled as a self-avoiding walk on a diamond lattice, with a potential of interaction of E, in units of k_BT, between total non-bonded neighbouring beads. Here k_B is Boltzmann's constant and T is the absolute temperature. The non-bonded interaction energy consists of interactions between solvent–solvent, segment–segment and solvent–segment pairs. The distance between two nearest-neighbours has a length of l_0 ($l_0^2 = 3$). Only the nearest-neighbour interactions are considered, and the conformations in which multiple occupancy of lattice sites occur are forbidden. The $\Delta\varepsilon_{\mathrm{pp}}$ (p, p$'$ = A or B) measures the energy of a polymer–solvent contact $\varepsilon_{\mathrm{ps}}$ relative to the energies of polymer–polymer $\varepsilon_{\mathrm{pp}}$ and solvent–solvent $\varepsilon_{\mathrm{ss}}$ contacts. Thus,

$$\Delta\varepsilon_{\mathrm{pp}} = \varepsilon_{\mathrm{pp}} + \varepsilon_{\mathrm{ss}} - \varepsilon_{\mathrm{ps}} - \varepsilon_{\mathrm{p's}} \qquad (1)$$

$\Delta\varepsilon_{\mathrm{pp}} = 0$ represents an athermal system where there is no resulting energy change upon the formation of a segment–segment pair. If $\Delta\varepsilon_{\mathrm{pp}}$ is very negative, it describes a polymer in a poor solvent, which means that polymer–polymer contacts are favoured, leading to a collapse in the chain dimensions at low temperatures. The total interaction energy of a system, E, can be obtained as the sum of all the pair-wise interactions corresponding to the various species as

$$E = N_{\mathrm{AA}}\Delta\varepsilon_{\mathrm{AA}} + N_{\mathrm{BB}}\Delta\varepsilon_{\mathrm{BB}} + N_{\mathrm{AB}}\Delta\varepsilon_{\mathrm{AB}} \qquad (2)$$

where N_{AA}, N_{BB} and N_{AB} are the number of non-bonded A–A, B–B and A–B nearest-neighbour segments respectively.

The algorithm used was the single-bond rotation or pivot algorithm, first introduced by Lal[27] and analysed thoroughly by Madras and Sokal[28]. This system has been treated by many authors and we have simply applied it in a block copolymer and sought to conduct rather long runs and thereby improve the accuracy. Using the Metropolis importance sampling scheme, the conformations in the limit of a large sample occur with a frequency proportional to their Boltzmann factor. Therefore, the estimated mean value of conformational property $\langle A\rangle$ over the canonical ensemble, is given by

$$\langle A\rangle = \frac{1}{K - K_0}\sum_{i=K_0+1}^{K} A(\mathbf{X}_i) \qquad (3)$$

where $A(\mathbf{X}_i)$ is the value of the property for configuration $\mathbf{X}_i$ and K is the number of configurations in the sample. In order to avoid a systematic error due to incomplete equilibration, the value of K_0 is carefully chosen.

The mean-square end-to-end distance $\langle R^2\rangle$ of the chain is calculated from a simple average over the sample of configurations, i.e.

$$\langle R^2\rangle = \frac{1}{K - K_0}\sum_{i=K_0+1}^{K} [\mathbf{R}_i(1) - \mathbf{R}_i(n)]^2 \qquad (4)$$

where the values of $\mathbf{R}_i(1)$ and $\mathbf{R}_i(n)$ are the end segment coordinates of the chain in a configuration $\mathbf{X}_i$. The mean-square radius of gyration $\langle R_{\mathrm{g}}^2\rangle$ is written as

$$\langle R_{\mathrm{g}}^2\rangle = \frac{1}{K - K_0}\sum_{i=K_0+1}^{K} R_{\mathrm{g}}^2(\mathbf{X}_i) \qquad (5)$$

where

$$R_{\mathrm{g}}^2(\mathbf{X}_i) = \frac{1}{(1+n)^2}\sum_{i=1}^{n}\sum_{j=\mathrm{i}}^{n+1} r_{ij}^2$$

and r_{ij} is the distance between beads i and j. The mean heat capacity $\langle C_{\mathrm{v}}\rangle$ is given by

$$-k_{\mathrm{B}}T^2\langle C_{\mathrm{v}}\rangle = \left(\frac{\sum_{i=K_0+1}^{K} E(\mathbf{X}_i)}{K - K_0}\right)^2 - \left(\frac{\sum_{i=K_0+1}^{K} [E(\mathbf{X}_i)]^2}{K - K_0}\right) \qquad (6)$$

The statistical errors were estimated by dividing the reduced sample of configurations into k sub-samples and assuming that the estimates given by the sub-samples are uncorrelated.

THE SELF-CONSISTENT FIELD THEORY

It has been shown by Edwards[29] that the conformations of a flexible chain can be related to the possible paths of a non relativistic particle in quantum mechanics. The SCF approach in polymer physics is related to Flory's mean field concept. An average is made over all segments of a polymer chain to produce an excluded volume field restricting the placement of each segment. The object of SCF theory is to self-consistently determine this mean field. With the modified Edwards Hamiltonian for polymers, we have extended the self-consistent field (SCF) approach to deal with the behaviour of a polymer both in good and bad solvents[30] and to account for the micellization of diblock copolymers in selective solvents[8].

Let us consider the diblock copolymer formed by connecting a block A of length L_{A} to a block B of length L_{B}. The total contour length, L, of the diblock copolymer chain is thus given by $L = L_{\mathrm{A}} + L_{\mathrm{B}}$. The short range interactions between segments in a diblock copolymer can be coarse grained into the statistical Kuhn lengths b_{A} and b_{B}. The additional difficulty in calculating the properties of a copolymer arises from the presence of three interaction parameters, i.e. interactions between A–A segments v_{AA}, B–B segments v_{BB} and A–B segments v_{AB}. If we fix the initial segment of the A block at the origin, the other end of the A block (the join with the B block) at the space point $\mathbf{R}_{\mathrm{J}}$ and the unattached end of the B block at $\mathbf{R}_\mathrm{B}$, the partition function for all possible conformations of the copolymer is given within the SCF approximation by

$$\Omega_\mathrm{C}(L_\mathrm{A}, L_\mathrm{B}) = \int \mathrm{d}\mathbf{R}_\mathrm{J}\mathrm{d}\mathbf{R}_\mathrm{B} G_\mathrm{c}(\mathbf{R}_\mathrm{B}, \mathbf{R}_\mathrm{J}, 0; L_\mathrm{B}, L_\mathrm{A}, 0) \tag{7a}$$

$$= \int \mathrm{d}\mathbf{R}_\mathrm{J}\mathrm{d}\mathbf{R}_\mathrm{B} G_\mathrm{A}(\mathbf{R}_\mathrm{J}, 0; L_\mathrm{A}, 0) G_\mathrm{B}(\mathbf{R}_\mathrm{B}, \mathbf{R}_\mathrm{J}; L_\mathrm{B}, 0) \tag{7b}$$

where the Greens functions G_A and G_B in equation (7b) satisfy the following SCF equations

$$\left[\frac{\partial}{\partial \tau_\mathrm{A}} - \frac{b_\mathrm{A}}{6}\nabla_\mathbf{R}^2 + \beta\omega_\mathrm{A}(\mathbf{R})\right] G_\mathrm{A}(\mathbf{R}, 0; \tau_\mathrm{A}, 0) = \delta(\mathbf{R})\delta(\tau_\mathrm{A})$$

$$(0 < \tau_\mathrm{A} \leqslant L_\mathrm{A}) \tag{8}$$

and

$$\left[\frac{\partial}{\partial \tau_\mathrm{B}} - \frac{b_\mathrm{B}}{6}\nabla_\mathbf{R}^2 + \beta\omega_\mathrm{B}(\mathbf{R})\right] G_\mathrm{B}(\mathbf{R}, \mathbf{R}_\mathrm{J}; \tau_\mathrm{B}, 0) = \delta(\mathbf{R} - \mathbf{R}_\mathrm{J})\delta(\tau_\mathrm{B})$$

$$(0 < \tau_\mathrm{B} \leqslant L_\mathrm{B}) \tag{9}$$

where $\beta = 1/k_\mathrm{B}T$. In order to approximate the interactions between A–A segments, B–B segments and A–B segments, the potentials of mean force in equations (8) and (9) for a diblock copolymer chain are taken to be given by

$$\beta\omega_\mathrm{A}(\mathbf{R}) = -\{\ln[1 - v_{0\mathrm{A}}\rho_\mathrm{A}(\mathbf{R}) - v_{0\mathrm{B}}\rho_\mathrm{B}(\mathbf{R})] + 2\chi_\mathrm{AA}v_{0\mathrm{A}}(\mathbf{R}) + 2\chi_\mathrm{AB}v_{0\mathrm{B}}\rho_\mathrm{B}(\mathbf{R})\}/b_\mathrm{A} \tag{10}$$

and

$$\beta\omega_\mathrm{B}(\mathbf{R}) = -\{\ln[1 - v_{0\mathrm{A}}\rho_\mathrm{A}(\mathbf{R}) - v_{0\mathrm{B}}\rho_\mathrm{B}(\mathbf{R})] + 2\chi_\mathrm{BB}v_{0\mathrm{B}}\rho_\mathrm{B}(\mathbf{R}) + 2\chi_\mathrm{AB}v_{0\mathrm{A}}\rho_\mathrm{A}(\mathbf{R})\}/b_\mathrm{B} \tag{11}$$

where $v_{0\mathrm{p}}$ ($\rho, \rho' = \mathrm{A}$ or B) are the segment hard core volumes of the A and B segments respectively and $\chi_{\mathrm{pp}'}$ are the Flory's interaction parameters between segments. The logarithm terms remedy the problems of the unphysically high segment densities for the original SCF equations[31–34] when the second virial coefficient between segments becomes negative, i.e. $v = v_0(1 - 2\chi)$ and $\chi < 0.5$. It treats approximately the hard core potential and the remaining terms treat the effects of the attractive forces. No doubt better forms for $\omega_\mathrm{p}(\mathbf{R})$ can be found, drawing for example on the density functional theory of liquids, but here we just use the simple form given above. $\rho_\mathrm{A}(\mathbf{R})$ and $\rho_\mathrm{B}(\mathbf{R})$ are the density distribution functions of the A and B segments respectively, which may be written as

$$\rho_\mathrm{A}(\mathbf{R}) = \frac{\int_0^{L_\mathrm{A}} \mathrm{d}\tau_\mathrm{A} G_\mathrm{A}(\mathbf{R}, 0; \tau_\mathrm{A}, 0) \int \mathrm{d}\mathbf{R}_\mathrm{J}\mathrm{d}\mathbf{R}_\mathrm{B} G_\mathrm{A}(\mathbf{R}_\mathrm{J}, \mathbf{R}; L_\mathrm{A}, \tau_\mathrm{A}) G_\mathrm{B}(\mathbf{R}_\mathrm{B}, \mathbf{R}_\mathrm{J}; L_\mathrm{B}, 0)}{\Omega_\mathrm{c}(L_\mathrm{A}, L_\mathrm{B})} \tag{12}$$

and

$$\rho_\mathrm{B}(\mathbf{R}) = \frac{\int_0^{L_\mathrm{B}} \mathrm{d}\tau_\mathrm{B} \int \mathrm{d}\mathbf{R}_\mathrm{J}\mathrm{d}\mathbf{R}_\mathrm{B} G_\mathrm{A}(\mathbf{R}_\mathrm{J}, 0; L_\mathrm{A}, 0) G_\mathrm{B}(\mathbf{R}, \mathbf{R}_\mathrm{J}; \tau_\mathrm{B}, 0) G_\mathrm{B}(\mathbf{R}_\mathrm{B}, \mathbf{R}; L_\mathrm{B}, \tau_\mathrm{B})}{\Omega_\mathrm{c}(L_\mathrm{A}, L_\mathrm{B})} \tag{13}$$

If we define the additional Green's functions

$$q_\mathrm{B}(\mathbf{R}; L_\mathrm{B}, \tau_\mathrm{B}) = \int \mathrm{d}\mathbf{R}' G_\mathrm{B}(\mathbf{R}', \mathbf{R}; L_\mathrm{B}, \tau_\mathrm{B}), \tag{14}$$

$$H_\mathrm{A}(\mathbf{R}; L_\mathrm{B}, \tau_\mathrm{A}) = \int \mathrm{d}\mathbf{R}_\mathrm{J}\mathrm{d}\mathbf{R}_\mathrm{B} G_\mathrm{A}(\mathbf{R}_\mathrm{J}, \mathbf{R}; L_\mathrm{A}, \tau_\mathrm{A}) \times G_\mathrm{B}(\mathbf{R}_\mathrm{B}, \mathbf{R}_\mathrm{J}; L_\mathrm{B}, 0)$$

$$= \int \mathrm{d}\mathbf{R}_\mathrm{J} G_\mathrm{A}(\mathbf{R}_\mathrm{J}, \mathbf{R}; L_\mathrm{A}, \tau_\mathrm{A}) q_\mathrm{B}(\mathbf{R}_\mathrm{J}; L_\mathrm{B}, 0) \tag{15}$$

and

$$H_\mathrm{B}(\mathbf{R}; \tau_\mathrm{B}, L_\mathrm{A}) = \int \mathrm{d}\mathbf{R}_\mathrm{J} G_\mathrm{A}(\mathbf{R}_\mathrm{J}, 0; L_\mathrm{A}, 0) G_\mathrm{B}(\mathbf{R}, \mathbf{R}_\mathrm{J}; \tau_\mathrm{B}, 0) \tag{16}$$

then equations (16) and (17) can be rewritten as

$$\rho_\mathrm{A}(\mathbf{R}) = \frac{\int_0^{L_\mathrm{A}} \mathrm{d}\tau_\mathrm{A} G_\mathrm{A}(\mathbf{R}, 0; \tau_\mathrm{A}, 0) H_\mathrm{A}(\mathbf{R}; L_\mathrm{B}, \tau_\mathrm{A})}{\Omega_\mathrm{c}(L_\mathrm{A}, L_\mathrm{B})} \tag{17}$$

and

$$\rho_\mathrm{B}(\mathbf{R}) = \frac{\int_0^{L_\mathrm{B}} \mathrm{d}\tau_\mathrm{B} H_\mathrm{B}(\mathbf{R}; \tau_\mathrm{B}, L_\mathrm{A}) q_\mathrm{B}(\mathbf{R}; L_\mathrm{B}, \tau_\mathrm{B})}{\Omega_\mathrm{c}(L_\mathrm{A}, L_\mathrm{B})}. \tag{18}$$

From the definitions given by equations (14)–(16), we can derive the SCF equations,

$$\left[\frac{\partial}{\partial \tau_\mathrm{B}} - \frac{b_\mathrm{B}}{6}\nabla_\mathbf{R}^2 + \beta\omega_\mathrm{B}(\mathbf{R})\right] q_\mathrm{B}(\mathbf{R}; \tau_\mathrm{B}) = \delta(\tau_\mathrm{B})$$

$$(0 < \tau_\mathrm{B} \leqslant L_\mathrm{B}) \tag{19}$$

$$\left[\frac{\partial}{\partial \tau_\mathrm{A}} - \frac{b_\mathrm{A}}{6}\nabla_\mathbf{R}^2 + \beta\omega_\mathrm{A}(\mathbf{R})\right] H_\mathrm{A}(\mathbf{R}; L_\mathrm{B}, \tau_\mathrm{A}) = q_\mathrm{B}(\mathbf{R}; L_\mathrm{B})\delta(\tau_\mathrm{A})$$

$$(0 < \tau_\mathrm{A} \leqslant L_\mathrm{A}) \tag{20}$$

and

$$\left[\frac{\partial}{\partial \tau_\mathrm{B}} - \frac{b_\mathrm{B}}{6}\nabla_\mathbf{R}^2 + \beta\omega_\mathrm{B}(\mathbf{R})\right] H_\mathrm{B}(\mathbf{R}; \tau_\mathrm{B}, L_\mathrm{A}) = G_\mathrm{A}(\mathbf{R}, 0; L_\mathrm{A}, 0)\delta(\tau_\mathrm{B})$$

$$(0 < \tau_\mathrm{B} \leqslant L_\mathrm{B}) \tag{21}$$

for the Green's functions $q_\mathrm{B}(\mathbf{R}; \tau_\mathrm{B}), H_\mathrm{A}(\mathbf{R}; L_\mathrm{B}, \tau_\mathrm{A})$ and $H_\mathrm{B}(\mathbf{R}; \tau_\mathrm{B}, L_\mathrm{A})$ respectively. Therefore, equations (7)–(11) and equations (17)–(21) are the closed set of SCF equations for a single diblock copolymer. If set $v_{0\mathrm{A}} = v_{0\mathrm{B}} = v_0$ and $\chi_\mathrm{AA} = \chi_\mathrm{BB} = \chi_\mathrm{AB} = \chi$, the SCF equations given above reduce to the case of a homopolymer chain[30].

Given the Green's functions $G_\mathrm{A}(\mathbf{R}_\mathrm{J}, 0; L_\mathrm{A}, 0)$, $q_\mathrm{B}(\mathbf{R}; \tau_\mathrm{B})$, $H_\mathrm{A}(\mathbf{R}; L_\mathrm{B}, \tau_\mathrm{A})$ and $H_\mathrm{B}(\mathbf{R}; \tau_\mathrm{B}, L_\mathrm{A})$, the Helmholtz free energy is calculated by

$$\beta F = -\ln\Omega_\mathrm{c}(L_\mathrm{A}, L_\mathrm{B}) - \frac{1}{2}\int \mathrm{d}\mathbf{R}[\omega_\mathrm{A}(\mathbf{R})\rho_\mathrm{A}(\mathbf{R}) + \omega_\mathrm{B}(\mathbf{R})\rho_\mathrm{B}(\mathbf{R})] \tag{22}$$

The mean-square end-to-end distance $\langle R^2 \rangle$ is given by

$$\langle R^2 \rangle = \frac{\int \mathrm{d}\mathbf{R}\mathbf{R}^2 \int G_\mathrm{A}(\mathbf{R}_\mathrm{J}, 0; L_\mathrm{A}, 0) G_\mathrm{B}(\mathbf{R}, \mathbf{R}_\mathrm{J}; L_\mathrm{B}, L_\mathrm{A}) \mathrm{d}\mathbf{R}_\mathrm{J}}{\Omega_\mathrm{C}(L_\mathrm{A}, L_\mathrm{B})} \tag{23}$$

The mean-square end-to-end distances of block A and block B respectively are given by

$$\langle R^2\rangle_A = \frac{\int \mathrm{d}\mathbf{R}\mathbf{R}^2 G_A(\mathbf{R},0;L_A,0)\int G_B(\mathbf{R}_B,\mathbf{R};L_B,L_A)\mathrm{d}\mathbf{R}_B}{\Omega(L_A,L_B)} \tag{24}$$

and

$$\langle R^2\rangle_B = \frac{\int \mathrm{d}\mathbf{R}_J \mathrm{d}\mathbf{R}_B G_A(\mathbf{R}_J,0;L_A,0)G_B(\mathbf{R}_B,\mathbf{R}_J;L_B,L_A)(\mathbf{R}_B-\mathbf{R}_J)^2}{\Omega_c(L_A,L_B)} \tag{25}$$

In order to simplify the SCF equations, we assume here the A and B segment densities are spherically symmetric about the origin. For a single-chain micelle, the spherical assumption might not be too bad. It is most clearly wrong in the limit of a homopolymer chain, where the behaviour of the inter half differs from that of the outer half. However, the spherical symmetry does permit a straightforward numerical solution of the equations and we hope that, in spite of the faults with the assumption, a test of how well it performs in practice will be of some benefit. Thus $\nabla^2 G$ reduces to

$$\frac{\partial^2 G}{\partial r^2} + \left(\frac{2}{r}\right)\frac{\partial G}{\partial r}$$

and the vector $\mathbf{R}$ reduces to the scalar r. The variables r_∞, L_A and $L_A + L_B$ are discretized as

$$r = i\Delta r \quad (i = 1,\ldots,N_r) \quad \text{and} \quad r_\infty = N_r\Delta r \tag{26a}$$

$$\tau_A = j_A\Delta\tau_A \quad (j_A = 0,\ldots,n_A) \quad \text{and} \quad L_A = n_A\Delta\tau_A \tag{26b}$$

$$\tau_B = j_B\Delta\tau_B \quad (j_B = 0,\ldots,n_B) \quad \text{and} \quad L_B = n_B\Delta\tau_B \tag{26c}$$

Here, $i = 0$ and $j_A = 0$ denote that the A block had its unattached end segment fixed at the origin. The initial conditions and boundary conditions for the copolymer SCF equations are

$$G_A(1,1) = \frac{1}{4\pi r^2\Delta r} \quad \text{and} \quad G_A(i,1) = 0 \quad (i = 2,\ldots,N_r) \tag{27a}$$

$$q_B(i,0) = 1 \qquad (i = 1,\ldots,N_r) \tag{27b}$$

$$H_A(i,1) = q_B(i,n_B) \quad (i = 1,2,\ldots,N_r) \tag{27c}$$

$$H_B(i,0) = G_A(i,n_A) \quad (i = 1,2,\ldots,N_r) \tag{27d}$$

and

$$G_A(N_r,j_A) = 0 \qquad (j_A = 0,1,2,\ldots,n_A) \tag{28a}$$

$$q_B(N_r,j_B) = 1 \qquad (j_B = 0,1,\ldots,n_B) \tag{28b}$$

$$H_A(N_r,j_A) = 0 \qquad (j_A = 0,1,2,\ldots,n_A) \tag{28c}$$

$$H_B(N_r,j_B) = 0 \qquad (j_B = 0,1,2,\ldots,n_B) \tag{28d}$$

Discrete versions of the SCF equations can be obtained by using the implicit Crank–Nicholson scheme[7].

To numerically solve the SCF equations, we begin with a guess for the density distributions of the A and B blocks were Gaussian distribution (ideal chain densities) and then make an initial guess for $\omega_A(i)$ and $\omega_B(i)$. The Crank–Nicholson scheme then permits the calculation of $G_A(i,j_A), q_B(i,j_B), H_A(N_r,j_A)$ and $H_B(N_r,j_B)$. The new density profile $\rho_A^*(i)$ and $\rho_B^*(i)$ can thereby be calculated by equations (17) and (18). Thus new estimates of $\omega_A^*(i)$ and $\omega_B^*(i)$ can be obtained from equations (10) and (11). We then repeat the iteration with a new guess

$$\omega_X^{\text{new}}(i) = \omega_X(i) + \lambda[\omega_X^*(i) - \omega_X(i)]$$

where λ is some relaxation parameter which typically falls between 0.70 and 0.95. This SCF iteration procedure is continued until the self-consistency condition

$$\max|\omega_X(i) - \omega_X^*(i)| \leqslant \varepsilon \quad (i = 1,2,\ldots,N_r)$$

is achieved. A value of $\varepsilon = 10^{-6}$ is used.

SEGREGATION TRANSITION OF A BLOCK COPOLYMER CHAIN

In this section, we investigate how the conformations of a block copolymer chain change as the interaction parameters vary, using both MC simulations and SCF calculations. Then, using only MC simulations, we explore the conformations of the collapsed dumbbell form of diblock copolymer chains and the segregation transition of triblock copolymer chains. Typically the chain was given between 2×10^5–5×10^5 moves for equilibration in our simulations, and between 10^6–5×10^6 moves to calculate averages. The errors were estimated by considering sub samples, each of 5×10^4–10^5 moves. For very negative values $\Delta\varepsilon$ the results were also checked in certain cases by conducting several, independent runs, equilibrating from different initial configurations.

Segregation in diblock copolymer chains

The AB diblock copolymer lattice chain which we were modelling contains 76 A segments and 76 B segments. In the MC simulation, we firstly fixed $\Delta\varepsilon_{BB} = 0$, and calculated various properties with different values of $\Delta\varepsilon_{AA}$ and $\Delta\varepsilon_{AB}$. These results are presented in *Table 1*. $\langle N_{AA}\rangle$ is defined as the average number of A–A neighbour contacts, and similarly for $\langle N_{BB}\rangle$ and $\langle N_{AB}\rangle$. For $\Delta\varepsilon_{BB} = \Delta\varepsilon_{AB} = 0$ and $\Delta\varepsilon_{AA}$ going from 0 to -0.8, $\langle N_{AA}\rangle$ increases and the mean-square radius of gyration of the A block decreases. The A block chain crosses over from the coil to the globule state whereas the conformations of the B block remain approximately unchanged. It stays in the coil state and is extended in the solvent. When we fixed $\Delta\varepsilon_{AA} = -0.8$ and $\Delta\varepsilon_{BB} = 0$ and varied $\Delta\varepsilon_{AB}$ from 0 to -0.8, as presented in *Table 1*, $\langle N_{AA}\rangle$ and $\langle N_{BB}\rangle$ remain virtually unchanged, i.e. the A block chain is in the globule state and the B block chain is still in the coil state. However, $\langle N_{AB}\rangle$ rapidly increases when $\Delta\varepsilon_{AB} < -0.5$ and the mean-square radius of gyration of A segments and B segments decreases slightly. This means that the configuration of the B block chain is changed from being extended and directed away from the A block segments to being still extended, but surrounding the A block segments. Snap-shot pictures taken from the simulation confirm this interpretation.

In order to carry out SCF calculations, we took the Flory prescription,

$$l = l_0\sqrt{6} \tag{29}$$

and

$$n = n_0/3 \tag{30}$$

which, in the absence of excluded volume effects, maps the tetrahedrally bonded 'real chain' onto an equivalent Gaussian chain of the same contour length. Here n_0 and b_0 are the number of bonds and the bond length respectively for the 'real' model chain. In our early SCF calculations for the homopolymer[30], fairly good agreement between MC simulation and SCF calculation was found by letting

$$v_0 = [-0.45 + 0.72 \times \ln(n)]l_0^3 \tag{31a}$$

and

$$\chi = 1.204 \times (-\Delta\varepsilon) \tag{31b}$$

The same transformation procedure has been taken in our SCF calculation for the above two stage segregation transitions. The mean-square end-to-end distances of the MC simulation and SCF calculation are presented in *Table 1*. It can be seen that the results of these two methods are in reasonable agreement for a wide range of solvent conditions.

Collapsed dumbbell form of diblock chains

We simulated the same chain as above, but this time we put $\Delta\varepsilon_{AA} = -0.8$, $\Delta\varepsilon_{BB} = -0.8$ and let $\Delta\varepsilon_{AB}$ vary between 0 and -0.8. The results are presented in *Table 2*. As can be seen, $\langle N_{AA}\rangle$ and $\langle N_{BB}\rangle$, and the mean-square radius of gyration of block A, $\langle R_g^2\rangle_A$, and block B, $\langle R_g^2\rangle_B$, are almost unchanged. This means both the conformations of block A and block B stay in the globule state when $\Delta\varepsilon_{AB}$ varies. However, $\langle N_{AB}\rangle$ rapidly increases for $\Delta\varepsilon_{AB}$ below the θ point and the mean-square distance between the centres of masses of the blocks A and B, $\langle d_{AB}^2\rangle$, decreases. This is in keeping with the idea that for $\Delta\varepsilon_{AB}$ above the θ point, the copolymer is in a collapsed dumbbell form, but when $\Delta\varepsilon_{AB}$ becomes more negative, the lobes start to fuse together to form one globule state like that of a homopolymer. The uniform conformation is in a globule state here rather than in the random flight state treated by Edwards[16].

By setting the interaction parameters as $\Delta\varepsilon_{AA} = \Delta\varepsilon_{BB} = \Delta\varepsilon_\theta + \Delta\varepsilon$ and $\Delta\varepsilon_{AB} = -\Delta\varepsilon_\theta - \Delta\varepsilon$ ($\Delta\varepsilon_\theta = -0.5$ at the Flory θ point), we simulated an AB lattice chain with three different lengths for the Edwards' special case where the segment interaction parameters $v_{AA} = v_{BB} = -v_{AB}$. The details of simulation results for $N_A = N_B = 126$ are also presented in *Table 2*. In fact, the case is much more complicated than the earlier one because of the way the interaction parameters were set. As $\Delta\varepsilon$ increases from -0.3 to 0.3, the chain changes from a collapsed dumbbell form to the random flight state at the θ point ($\Delta\varepsilon = 0$), then to a wring state in which two blocks of the chain wring together. The distance between the mass centres of block A and B, $\langle d_{AB}^2\rangle/l_0^2$, has a maximum at $\Delta\varepsilon = 0$, where the chain is a homopolymer and in the θ condition. As $\Delta\varepsilon$ becomes negative, both block A and B are shrunken in size and thus $\langle d_{AB}^2\rangle/l_0^2$ decreases. On the other hand, for positive $\Delta\varepsilon$, $\langle N_{AB}\rangle$ increases sharply and the sizes of A and B block keep approximately the same. This fusing of block A and B makes smaller $\langle d_{AB}^2\rangle/l_0^2$. The average number of A–B neighbour contacts $\langle N_{AB}\rangle$ is plotted against $\Delta\varepsilon$ in *Figure 1* for the three different lengths of chains. As expected, the longer the chain length is, the sharper the phase transition. However, our results still fall short to give the important information on the order of the transition and on the critical temperature due to the limited size of the simulation system and the poor statistical sampling scheme as $|\Delta\varepsilon|$ becomes bigger. We hope to return to this problem in future work.

Table 1 Segregations in diblock copolymer chain

$\Delta\varepsilon_{BB} = 0$ $\Delta\varepsilon_{AB} = 0$ $n_A = n_B = 76$							
$\Delta\varepsilon_{AA}$	$\langle N_{AA}\rangle$	$\langle N_{BB}\rangle$	$\langle N_{AB}\rangle$	$\langle R_g^2\rangle_A/l_0^2$	$\langle R_g^2\rangle_B/l_0^2$	$(\langle R^2\rangle/l_0^2)_{MC}$	$(\langle R^2\rangle/l_0^2)_{SCF}$
0.0	4.20 ± 0.03	4.08 ± 0.02	0.69 ± 0.01	36.3 ± 0.11	35.9 ± 0.12	515 ± 1.3	501.7
-0.1	4.78 ± 0.04	4.09 ± 0.03	0.70 ± 0.01	34.8 ± 0.14	35.7 ± 0.09	502 ± 1.7	495.3
-0.2	5.52 ± 0.04	4.11 ± 0.03	0.69 ± 0.01	33.3 ± 0.14	35.8 ± 0.10	494 ± 1.2	486.0
-0.3	6.54 ± 0.04	4.08 ± 0.03	0.72 ± 0.01	31.2 ± 0.13	36.0 ± 0.15	480 ± 1.9	475.4
-0.4	7.9 ± 0.1	4.07 ± 0.03	0.72 ± 0.01	28.8 ± 0.16	35.9 ± 0.15	459 ± 1.7	462.9
-0.5	9.3 ± 0.1	4.10 ± 0.04	0.73 ± 0.02	26.3 ± 0.19	35.9 ± 0.13	442 ± 2.1	448.9
-0.6	11.3 ± 0.2	4.07 ± 0.04	0.73 ± 0.01	23.1 ± 0.27	35.8 ± 0.11	417 ± 2.2	432.9
-0.7	13.7 ± 0.15	4.04 ± 0.03	0.77 ± 0.01	20.1 ± 0.18	36.2 ± 0.14	395 ± 2.4	413.0
-0.8	17.1 ± 0.34	4.08 ± 0.03	0.78 ± 0.02	16.5 ± 0.28	35.9 ± 0.10	365 ± 2.7	383.6
$\Delta\varepsilon_{AA} = -0.8$ $\Delta\varepsilon_{BB} = 0$ $n_A = n_B = 76$							
$\Delta\varepsilon_{AB}$	$\langle N_{AA}\rangle$	$\langle N_{BB}\rangle$	$\langle N_{AB}\rangle$	$\langle R_g^2\rangle_A/l_0^2$	$\langle R_g^2\rangle_B/l_0^2$	$(\langle R^2\rangle/l_0^2)_{MC}$	$(\langle R^2\rangle/l_0^2)_{SCF}$
-0.1	16.6 ± 0.3	4.07 ± 0.03	1.02 ± 0.03	16.7 ± 0.3	35.9 ± 0.09	362 ± 2.0	377.0
-0.2	16.2 ± 0.3	4.03 ± 0.03	1.17 ± 0.03	17.2 ± 0.3	35.9 ± 0.09	361 ± 2.4	367.1
-0.3	16.4 ± 0.2	4.06 ± 0.04	1.61 ± 0.03	17.1 ± 0.2	35.8 ± 0.1	350 ± 1.8	355.2
-0.4	17.2 ± 0.4	4.16 ± 0.04	2.13 ± 0.04	16.2 ± 0.3	35.3 ± 0.1	330 ± 2.5	340.2
-0.5	16.2 ± 0.4	4.16 ± 0.04	3.2 ± 0.1	16.9 ± 0.3	35.1 ± 0.2	314 ± 3.0	322.6
-0.6	16.9 ± 0.2	4.14 ± 0.03	4.8 ± 0.1	16.1 ± 0.2	34.2 ± 0.1	283 ± 2.2	302.5
-0.7	16.7 ± 0.3	4.31 ± 0.04	7.8 ± 0.3	15.9 ± 0.2	32.6 ± 0.2	239 ± 3.0	278.8
-0.8	16.5 ± 0.4	4.61 ± 0.09	14.2 ± 0.7	14.8 ± 0.3	29.1 ± 0.4	179 ± 4.6	245.8

Table 2 Collapsed dumbbell form of diblock chain

$\Delta\varepsilon_{AA} = -0.8$ $\Delta\varepsilon_{BB} = -0.8$ $n_A = n_B = 76$ $\Delta\varepsilon_{AB}$	$\langle N_{AA}\rangle$	$\langle N_{BB}\rangle$	$\langle N_{AB}\rangle$	$\langle R_g^2\rangle_A/l_0^2$	$\langle R_g^2\rangle_B/l_0^2$	$\langle R^2\rangle/l_0^2$	$\langle d_{AB}^2\rangle/l_0^2$
0.0	16.8 ± 0.2	15.9 ± 0.2	0.89 ± 0.01	16.7 ± 0.2	17.1 ± 0.2	226 ± 2.2	296 ± 1.9
−0.1	16.7 ± 0.3	16.4 ± 0.2	1.11 ± 0.02	16.8 ± 0.2	16.6 ± 0.2	220 ± 2.1	286 ± 2.4
−0.2	16.6 ± 0.2	16.5 ± 0.2	1.46 ± 0.03	17.0 ± 0.2	16.6 ± 0.2	217 ± 1.9	275 ± 2.3
−0.3	16.0 ± 0.2	16.2 ± 0.3	1.86 ± 0.04	17.4 ± 0.2	16.7 ± 0.2	214 ± 2.1	266 ± 2.3
−0.4	16.6 ± 0.2	16.2 ± 0.2	2.55 ± 0.06	16.7 ± 0.2	16.8 ± 0.2	200 ± 1.6	244 ± 1.6
−0.5	16.9 ± 0.1	16.0 ± 0.2	3.6 ± 0.1	16.4 ± 0.1	16.8 ± 0.2	185 ± 1.4	217 ± 2.0
−0.6	16.4 ± 0.2	16.7 ± 0.2	5.2 ± 0.2	16.4 ± 0.2	15.8 ± 0.2	165 ± 2.2	183 ± 3.1
−0.7	16.5 ± 0.4	16.4 ± 0.3	9.0 ± 0.5	15.8 ± 0.3	15.7 ± 0.3	136 ± 3.1	135 ± 4.5
−0.8	15.9 ± 0.3	16.5 ± 0.4	12.9 ± 0.6	15.6 ± 0.3	15.0 ± 0.3	110 ± 3.0	91 ± 4.1
$\Delta\varepsilon_{AA} = \Delta\varepsilon_{BB} = -0.5 + \Delta\varepsilon$ $\Delta\varepsilon_{AB} = -0.5 - \Delta\varepsilon$ $n_A = n_B = 126$ $\Delta\varepsilon$	$\langle N_{AA}\rangle$	$\langle N_{BB}\rangle$	$\langle N_{AB}\rangle$	$\langle R_g^2\rangle_A/l_0^2$	$\langle R_g^2\rangle_B/l_0^2$	$\langle R^2\rangle/l_0^2$	$\langle d_{AB}^2\rangle/l_0^2$
−0.3	34.3 ± 0.6	34.4 ± 0.7	1.62 ± 0.03	22.4 ± 0.4	21.8 ± 0.5	279.8 ± 0.8	387 ± 4.8
−0.2	28.2 ± 0.6	28.9 ± 0.6	2.09 ± 0.05	28.5 ± 0.5	28.0 ± 0.5	360 ± 5.3	452 ± 6.0
−0.1	21.9 ± 0.3	22.4 ± 0.7	2.8 ± 0.1	36.2 ± 0.4	35.8 ± 0.8	451 ± 6.0	504 ± 6.9
0.0	17.6 ± 0.2	17.6 ± 0.3	4.6 ± 0.2	43.0 ± 0.4	42.6 ± 0.4	506 ± 5.3	511 ± 8.2
0.1	14.0 ± 0.2	14.5 ± 0.2	7.5 ± 0.5	47.4 ± 0.3	46.6 ± 0.6	501 ± 7.6	449 ± 11
0.2	12.3 ± 0.3	12.7 ± 0.4	16 ± 1	46.5 ± 0.9	46.6 ± 0.9	409 ± 14	291 ± 17
0.3	11.4 ± 0.5	12.1 ± 0.5	28 ± 2	42 ± 2.0	41 ± 2.0	286 ± 17	138 ± 18

Segregation transition in triblock copolymer chains

A triblock ABA lattice chain which comprises 45 A segments connected to 90 B segments followed by another 45 A segments, i.e. $N_{A1} = 45$, $N_B = 90$ and $N_{A2} = 45$, was simulated. We call the first A block A1 and the second A2. We set $\Delta\varepsilon_{BB} = 0$ and $\Delta\varepsilon_{AB} = -0.5$ and calculated the properties as one varied $\Delta\varepsilon_{AA}$. The results are presented in *Table 3*. The average neighbour contact number of non-bonded B–B segments, $\langle N_{BB}\rangle$, and A–B segments, $\langle N_{AB}\rangle$, are changed slightly when $\Delta\varepsilon_{AA}$ becomes more negative. But, the average neighbour contact number between A1 block segments and A2 block segments, $\langle N_{AA}\rangle_{12}$, rapidly increases for $\Delta\varepsilon_{AA} < -0.8$ and the mean-square distance between the centres of mass of the block A1 and the block A2, $\langle d_{AA}^2\rangle_{12}/b_0^2$, decreases rapidly. It should be noted that $\langle N_{AA}\rangle_1 \approx \langle N_{AA}\rangle_2$ in every transition stage and $\langle N_{AA}\rangle_1 \approx \langle N_{AA}\rangle_{12} \approx \langle N_{AA}\rangle_2$ at $\Delta\varepsilon_{AA} = -1.2$, i.e. A segments from different A blocks are entirely mixed together. This implies that a transition takes place from the state of two collapsed A globules at either end of the B chain to a state of one collapsed A globule with a loop of B chain sticking out. The peak in the heat capacity $\langle C_v\rangle$ and the sharp increase of the average number of A–A neighbour contacts between different A blocks $\langle N_{AA}\rangle_{12}$ shown in *Figure 2* are signs of the transition. The transition temperature here might be lower than the actual transition temperature due to a finite chain.

The transition is basically determined by a competition between the A–A segments desire to mix together (energy driven) and the B block chain's desire to be in an extended coil state (entropy driven). In the conformation of two collapsed A globules at either end of the B chain, the latter factor dominates. In the configurations having one collapsed A globule with a loop of B block chain sticking out, the former factor dominates. Of course, many more simulations are needed to map out the phase diagram in terms of the molecular parameters.

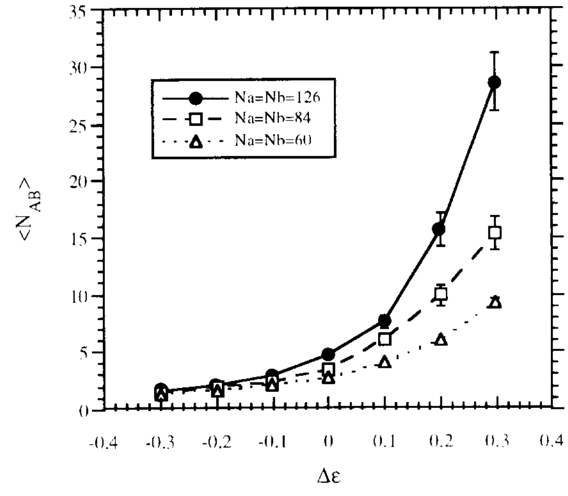

Figure 1 The average number of A–B neighbour contacts $\langle N_{AB}\rangle$ is plotted against $\Delta\varepsilon$

SUMMARY

We has developed a self-consistent field theory and a Monte Carlo simulation method for predicting the conformational properties of a block copolymer chain. The Monte Carlo simulations have served to check the validity of SCF theory and to explore new phenomena involving a single block copolymer chain.

The common conformations of diblock copolymer chains are of one block (A block) in a globule state (i.e. the solvent bad for A block segments) and the other block (B block) in a coil state (i.e. the solvent good for B block segments). A simple new mean-field potential, equations (14) and (15), was used to remedy the

Table 3 Segregation transition in triblock copolymer chain

$\Delta\varepsilon_{AB} = -0.5$ $\Delta\varepsilon_{BB} = 0$ $N_{A1} = 45$ $N_B = 90$ $N_{A2} = 45$

$\Delta\varepsilon_{AA}$	$\langle N_{AA}\rangle_{11}$	$\langle N_{AA}\rangle_{12}$	$\langle N_{AA}\rangle_{22}$	$\langle N_{BB}\rangle$	$\langle N_{AB}\rangle$	$\langle R^2\rangle/b_0^2$	$\langle d_{AA}^2\rangle_{12}/l_0^2$
−1.20	11.4 ± 0.3	11.7 ± 1.0	10.9 ± 0.4	5.5 ± 0.3	4.6 ± 0.3	99 ± 12.2	230 ± 37.2
−1.10	10.2 ± 0.3	10.7 ± 0.8	10.1 ± 0.3	6.8 ± 0.3	7.6 ± 0.5	116 ± 12.5	254 ± 39.6
−1.05	10.1 ± 0.1	5.5 ± 0.7	9.9 ± 0.2	5.8 ± 0.4	6.2 ± 0.3	208 ± 12.9	544 ± 38.1
−1.00	10.2 ± 0.2	4.3 ± 0.7	9.6 ± 0.2	5.2 ± 0.2	6.4 ± 0.3	244 ± 13.5	634 ± 40.9
−0.9	8.5 ± 0.1	2.2 ± 0.4	8.5 ± 0.2	5.2 ± 0.1	5.9 ± 0.3	312 ± 9.1	808 ± 27.3
−0.8	7.53 ± 0.07	1.0 ± 0.2	7.54 ± 0.08	5.05 ± 0.04	5.4 ± 0.1	364 ± 4.0	925 ± 11.7
−0.7	6.56 ± 0.06	0.7 ± 0.1	6.45 ± 0.06	5.10 ± 0.03	5.19 ± 0.08	393 ± 3.6	972 ± 10.3
−0.6	5.56 ± 0.04	0.30 ± 0.02	5.60 ± 0.04	5.06 ± 0.03	5.15 ± 0.06	426 ± 1.8	1032 ± 4.9

$\Delta\varepsilon_{AA}$	$\langle R^2\rangle_{A1}/l_0^2$	$\langle R^2\rangle_B/l_0^2$	$\langle R^2\rangle_{A2}/l_0^2$	$\langle R_g^2\rangle/l_0^2$	$\langle R_g^2\rangle_{A1}/l_0^2$	$\langle R_g^2\rangle_B/l_0^2$	$\langle R_g^2\rangle_{A2}/l_0^2$
−1.20	38 ± 1.8	96 ± 8.5	33 ± 2.3	37 ± 1.9	8.0 ± 0.2	32.6 ± 0.7	7.4 ± 0.2
−1.10	41 ± 2.3	87 ± 11.0	46 ± 2.4	35 ± 2.2	8.3 ± 0.2	32.1 ± 1.0	8.5 ± 0.3
−1.05	45 ± 1.3	171 ± 8.3	42 ± 1.2	51 ± 2.0	8.8 ± 0.1	36.9 ± 0.7	8.7 ± 0.1
−1.00	45 ± 1.2	188 ± 9.4	48 ± 1.2	56 ± 2.0	8.7 ± 0.2	37.7 ± 0.7	9.1 ± 0.1
−0.9	54 ± 1.2	226 ± 6.0	55 ± 1.0	64 ± 1.4	10.2 ± 0.1	40.0 ± 0.5	10.1 ± 0.1
−0.8	62.6 ± 0.6	249 ± 2.8	63 ± 0.7	70.5 ± 0.6	11.28 ± 0.07	41.7 ± 0.3	11.27 ± 0.09
−0.7	72.0 ± 0.5	256 ± 2.4	70.8 ± 0.6	73.6 ± 0.5	12.48 ± 0.07	42.3 ± 0.2	12.44 ± 0.07
−0.6	80.9 ± 0.5	267 ± 1.1	80.1 ± 0.4	77.1 ± 0.3	13.74 ± 0.06	42.9 ± 0.1	13.63 ± 0.06

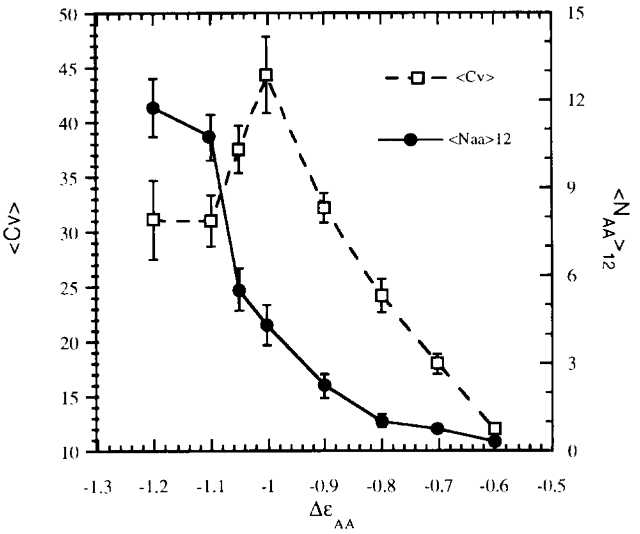

Figure 2 The average number of A–A neighbour contacts between different A blocks $\langle N_{AA}\rangle_{12}$ and the mean heat capacity $\langle C_v\rangle$ is plotted against $\Delta\varepsilon_{AA}$

problems of the unphysically high segment densities for the original SCF equations. The errors in the SCF calculations mainly arise from using an approximate Van der Waals like mean field, equations (14) and (15), and in the identification of the basic quantities of an equivalent Gaussian chain, such as the segment volume, the interaction parameter and the Kuhn statistical length, for polymers. In addition to these, the assumption of fixing one end at the origin is very crude. Nevertheless, using the relationships of $v_0 \sim n$ [equation (31a)] and $\chi \sim \Delta\varepsilon$ [equation (31b)], the mean-square end-to-end distances of a block copolymer calculated by SCF theory was found to be reasonably in agreement with the results from MC simulations. This suggests that our straightforward SCF calculation is of some benefit in practice. In our earlier publication on SCF calculations for micelle formation by block copolymers[8], the assumption of fixing one end at the origin has been relaxed and good agreement with experiments has also been achieved.

The segregation transitions of an AB diblock and an ABA triblock copolymer chain are modelled by MC simulation using the single bond rotation algorithm. We found a phase transition occurs between the chain having a spherical shape to it having dumbbell state, for the case of $L_A = L_B$ and by varying $\Delta\varepsilon_{AB}$ from −0.8 to 0.0 and fixing $\Delta\varepsilon_{AA} = \Delta\varepsilon_{BB} = -0.8$. However, for the Edwards' case of $v_{AA} = v_{BB} = -v_{AB}$, we have not obtained any conclusive result at present to indicate whether a phase transition exists. A sharp transition between two conformations has been observed for an ABA triblock copolymer chain in the case of $L_A = L_{A2}$ and $L_{A1} + L_{A2} = L_B$. When $\Delta\varepsilon_{BB} = 0.0$ and $\Delta\varepsilon_{AB} = -0.5$, varying $\Delta\varepsilon_{AA}$ from −0.6 to −1.20, leads to the occurrence of a phase transition: from two collapsed A globules at either end of the B chain to one collapsed A globule comprising of both A blocks with a loop of B chain sticking out. As the concentration of triblock copolymers in solutions increases, one conformation of a chain prefers to form itself into a micelle state while another intends to form a network. Thus, the studying of such a phase transition has great importance on the understanding of the viscoelastic properties of triblock copolymeric gels. We intend to carry out a more careful study on the subject in the future.

ACKNOWLEDGEMENTS

We are indebted to Dr M. Lal for providing us with the Monte Carlo simulation program for single homopolymer chain and to Dr M. Vincent for help with the computing. We have also benefited from many helpful discussions with Colin Price, Colin Booth, Sir Sam F. Edwards and R. Evans.

REFERENCES

1 Brown, R. A., Masters, A. J., Price, C. and Yuan, X.-F. 'Comprehensive Polymer Science' (Eds C. Booth and C. Price), 1989, Vol. 2, Chapter 6, Pergamon Press, Oxford, p. 155
2 Bates, F. S. and Fredrickson, G. H. *Annu. Rev. Phys. Chem.* 1990, **41**, 525
3 Luo, Y.-Z., Nicholas, C. V., Attwood, D., Collett, J. H., Price, C., Booth, C., Chu, B. and Zhou, Z.-K. *J. Chem. Soc. Faraday Trans.* 1993, **89**, 539; Nicholas, C. V., Luo, Y.-Z., Deng, N.-J., Attwood, D., Collett, J. H., Price, C. and Booth, C. *Polymer* 1993, **34**, 138
4 Wanka, G., Hoffmann, H. and Ulbricht, W. *Macromolecules* 1994, **27**, 4145; Almgren, M., Brown, W. and Hvidt, S. *Colloid Polym. Sci.* 1995, **273**, 2
5 Bates, F. S., Schulz, M. F., Khandpur, A. K., Forster, S., Rosedale, J. H., Almdal, K. and Mortensen, K. *Faraday Discuss.* 1994, **98**, 7
6 Helfand, E. *Macromolecules* 1975, **8**, 552; Helfand, E. and Wasserman, Z. R. *Macromolecules* 1976, **6**, 879
7 Hong, K. M. and Noolandi, J. *Macromolecules* 1981, **14**, 727
8 Yuan, X.-F., Masters, A. J. and Price, C. *Macromolecules* 1992, **25**, 6876
9 Shull, K. R., *Macromolecules* 1993, **26**, 2346
10 Linse, P. *Macromolecules* 1993, **26**, 4437
11 Whitmore, M. D. and Vavasour, J. D. *Macromolecules* 1992, **25**, 2041; Vavasour, J. D. and Whitmore, M. D. *Macromolecules* 1993, **26**, 7070
12 McConnell, G. A., Lin, E. K., Gast, A. P., Huang, J. S., Lin, M. Y. and Smith, S. D. *Faraday Discuss.* 1994, **98**, 121
13 Zhan, Y. J. and Mattice, W. L. *Macromolecules* 1994, **27**, 677; Nguyen-Misra, M. and Mattice, W. L. *Macromolecules* 1995, **28**, 1444
14 Froelich, O. and Benoit, H. *Makromol. Chem.* 1966, **92**, 224
15 Edwards, S. F. *J. Phys. A* 1974, **7**, 332
16 Bendler, J., Solc, K. and Gobusch, W. *Macromolecules* 1977, **10**, 635
17 Bendler, J. and Solc, K. *Polym. Eng. Sci.* 1977, **17**, 8
18 Bendler, J. and Solc, K. *Polym. Prepr., Am. Chem. Soc., Div. Polym. Chem.* 1977, **18**, 319
19 Tanaka, T., Kotaka, T. and Inagaki, H. *Macromolecules* 1976, **9**, 561
20 Tanaka, T., Kotaka, T., Ban, K., Hattori, M. and Inagaki, H. *Macromolecules* 1977, **10**, 960
21 Tanaka, T. and Kotaka, T. *Polym. Prepr., Am. Chem. Soc., Div. Polym. Chem.* 1979, **20**, 9
22 Tanaka, T., Omoto, M. and Inagaki, H. *Macromolecules* 1979, **21**, 147
23 Kimura, T. and Kurata, M. *J. Polym. Sci., Polym. Phys. Edn.* 1979, **17**, 2133
24 Joanny, J.-F., Leibler, L. and Ball, R. *J. Chem. Phys.* 1984, **81**, 4640
25 Douglas, J. F. and Freed, K. F. *J. Chem. Phys.* 1987, **86**, 4280
26 McMullen, W. E., Freed, K. F. and Cherayil, B. J. *Macromolecules* 1989, **22**, 1853
27 Lal, M. *Mol. Phys.* 1989, **17**, 57
28 Madras, N. and Sokal, A. D. *J. Stat. Phys.* 1988, **50**, 109
29 Edwards, S. F. *Proc. Phys. Soc.* 1965, **85**, 613
30 Yuan, X.-F. and Masters, A. J. *J. Chem. Phys.* 1991, **94**, 6908; Yuan, X.-F. 'SCF Theory and Computer Simulation of Copolymer Chains', PhD thesis, Manchester University, 1989
31 Dolan, A. K. and Edwards, S. F. *Proc. R. Soc. London, A* 1974, **337**, 509; 1975, **343**, 427
32 de Gennes, P. G. 'Scaling Concepts in Polymer Physics', Cornell University Press, Ithaca, New York, 1979
33 Doi, M. and Edwards, S. F. 'The Theory of Polymer Dynamics', Clarendon Press, Oxford, 1986
34 Freed, K. F. *Adv. Chem. Phys.* 1972, **22**, 1; 'Renormalization Group Theory of Macromolecules', Wiley, New York, 1987